Benzydamine, a CDK2 Kinase Inhibitor, Suppresses The Growth of Esophageal Squamous Cell Carcinoma in Vitro and in Vivo.

Yubing Zhou
Zhengzhou University
Xinyu He
Zhengzhou University
Yanan Jiang
Zhengzhou University
Zitong Wang
Zhengzhou University
Yin Yu
Zhengzhou University
Wenjie Wu
Zhengzhou University
Chenyang Zhang
Zhengzhou University
Jincheng Li
Zhengzhou University
Yaping Guo
Zhengzhou University
Xinhuan Chen
Zhengzhou University
Zhicai Liu
The Tumor Hospital of Linzhou City
Jimin Zhao
Zhengzhou University
Kangdong Liu (kdliu@zzu.edu.cn)
Zhengzhou University
Zigang Dong
Zhengzhou University

Research

Keywords: Benzydamine, CDK2, patient-derived xenograft, esophageal squamous cell carcinoma

Posted Date: May 7th, 2021

DOI: https://doi.org/10.21203/rs.3.rs-464145/v1

Abstract

Background: Esophageal squamous cell carcinoma (ESCC) is among one of the leading causes of cancer death worldwide owing to late detection and low survival rate. The clinical outcome of ESCC remains dismal. To date, the disease lacks available targeted therapies. Recently, drugs approved by the Food and Drug Administration have been reported to have potential as cancer chemoprevention agents.

Methods: Benzydamine, available as a hydrochloride salt, a locally acting non-steroidal anti-inflammatory drug, was screened out among FDA-approved drugs owing to its effective cytotoxic effect on KYSE450 cells, which remained unexplored. Mass spectrometry, kinase prediction and Swiss Target Prediction were used to verify the potential target(s) of benzydamine. Patient-derived oesophageal xenograft mouse model were used to investigate the effect of benzydamine on tumor growth *in vivo*.

Results: We found that benzydamine inhibited anchorage-dependent and -independent growth of ESCC cells. Kyoto Encyclopedia of Genes and Genomes pathway enrichment revealed that benzydamine attenuated five signaling pathways, including the DNA replication pathway. We further found that benzydamine could bind to CDK2 in its ATP-binding site. Inhibition of the activity of CDK2 suppressed the growth of ESCC cells and led to a G1/S cell cycle arrest. Additionally, knocking-down CDK2 decreased the sensitivity of ESCC cells to benzydamine hydrochloride. Notably, benzydamine suppressed tumour growth in a patient-derived oesophageal xenograft mouse model of ESCC *in vivo*.

Conclusions: We have identified CDK2 as a potential target of benzydamine for the treatment and prevention of ESCC. Benzydamine suppressed the growth of ESCC cells by inhibiting the activity of CDK2.

Background

Esophageal cancer (EC) is histopathologically classified into esophageal squamous cell carcinoma (ESCC) and esophageal adenocarcinoma [1]. It is estimated that 456 000 patients with ESCC exist worldwide, with approximately 90 % of them being found in Eastern and Central Asia [2]. Currently, a combination therapy of surgical resection, radiotherapy, and chemotherapy is the primary approach for the treatment of EC. However, the overall 5-year survival rate for advanced stage ESCC remains lower than 15 %, and the recurrence rate is still very high after treatment[3-5]. Therefore, it is urgent to identify effective drugs for the treatment of ESCC. Currently, chemoprevention is a new strategy which is widely used to reduce the onset of cancer and the relapse rate after treatment [6, 7]. Over the past few years, numerous drugs approved by the U.S. Food and Drug Administration (FDA) have been considered to be chemopreventive agents owing to their safety and pharmacodynamic characteristics [8] [9]. Among them, several non-steroidal anti-inflammatory drugs (NSAIDs) such as aspirin and ibuprofen have been widely reported in cancer chemoprevention [7]. By screening FDA-approved drugs, we found that benzydamine, a NSAID, could suppress the proliferation of ESCC cells. It has been shown to possess local anesthetic and analgesic properties [10]. However, its anti-tumor activity and underlying molecular mechanisms have not yet been elucidated.

Cyclin-dependent kinase 2 (CDK2) is considered to be a vital kinase in cell cycle regulation, participating in a series of biological processes. In many cancers, CDK2 plays an important role in tumor proliferation and correlated with cancer patients' survival [11, 12]. Additionally, emerging evidence has demonstrated that inhibition of CDK2 elicits an anti-tumor activity in a subset of tumors [13]. Therefore, CDK2-selective inhibitors might present a therapeutic opportunity for CDK2-highly expressed cancers [14]. In this study, we identified benzydamine, a FDA-approved drug, as a CDK2 inhibitor. We elucidated the anti-tumor effect of benzydamine in ESCC *in vitro* and *in vivo*, which was shown to be achieved through the attenuation of the CDK2/ minichromosome maintenance protein 2 (MCM2) signaling pathways. In sum up, our results suggested that targeting CDK2 is a potentially effective therapeutic strategy for improving the treatment of ESCC.

Materials And Methods

Reagents and antibodies

Benzydamine hydrochloride was purchased from J&K Scientific (CAS: 132-69-4; #375843, Beijing, China). CNBr-Sepharose 4B beads were purchased from GE Healthcare (Piscataway, NJ, USA). Fetal bovine serum (FBS), RPMI 1640 medium, and Dulbecco's Modified Eagle's medium (DMEM) were purchased from Biological Industries (Beit HaEmek, Israel). Antibodies against p-MCM2 (Ser41) (#ab109270), MCM2 (#ab108935), p-Rb (Thr826) (#ab133446), and Rb (#ab181616) were purchased from Abcam (Cambridge, England). Primary antibodies against p-c-Myc (Ser62) (#13748) and c-Myc (#9402) were purchased from Cell Signaling Technology (Danvers, MA, USA). The primary antibody against GAPDH (60004-1-Ig) was purchased from Proteintech Group (Wuhan, China).

Cell culture and cell lines

Shantou human embryonic esophageal (SHEE) cells were obtained from Enmin Li, Shantou University, Guangdong, China. The KYSE150 and KYSE450 ESCC cell lines were purchased from the Chinese Academy of Sciences Cell Bank (Shanghai, China). KYSE150 cells were cultured in RPMI 1640 medium containing 10 % FBS, 0.1 % penicillin (NCPC; North China Pharmaceutical, China), and 0.1 % streptomycin (Shandong Lukang Pharmaceutical Group, China). KYSE450 cells were grown in DMEM containing 10 % FBS, 0.1 % penicillin, and 0.1 % streptomycin. All cell lines were incubated at 37 °C and an atmosphere of 5 % CO_2 in a sterile incubator.

Cell proliferation assay

SHEE (2×10^3 cells/well), KYSE150 (3×10^3 cells/well), and KYSE450 (5×10^3 cells/well) cells were seeded in 96-well plates and cultured for 16–18 h. Various concentrations of benzydamine (0, 2.5, 5, 10, and 20 μM) were added to the cells. The nuclei of cells were stained with 4', 6-diamidino-2-phenylindole, and the cells were counted at various time points (0, 24, 48, 72, and 96 h) using an IN Cell Analyzer 6000 software.

Anchorage-independent cell growth assay

KYSE150 and KYSE450 cells (8×10^3 cells/well) were suspended in RPMI 1640 and DMEM containing 0.3 % agar and 10 % FBS at various concentrations of benzydamine (0, 2.5, 5, 10, and 20 μM). Cells were cultured at 37 °C and 5 % CO_2 for 10 days. Colonies were measured and analyzed using the IN Cell Analyzer 6000 software.

Plate cloning assay

KYSE150 and KYSE450 cells (3×10^2 cells/well) were suspended in 6-well plates containing various doses of benzydamine (0, 2.5, 5, 10, and 20 μM) for 10 days. Then, 0.3 % crystal violet (Solarbio, Beijing, China) was used for staining clones for 4 min. Colonies were counted and photographed.

Cell sample preparation and phosphoproteomics analysis

KYSE150 cells (4.5×10^6) were seeded in 15 cm dishes. After 16–18 h of culture followed by 20 μM benzydamine treatment for 24 h, cells were lysed in lysis buffer (RIPA lysate, Solarbio, Beijing, China, #R0020). After centrifuging the samples to remove debris, the supernatant was collected. The samples were digested with trypsin and the tryptic peptides were fractionated by high pH reverse-phase HPLC using a Thermo Betasil C18 column (5 μm particles, 10 mm ID, 250 mm length). In brief, peptides were separated with a gradient of 8–32 % acetonitrile (pH 9.0) for approximately 60 min, resulting in 60 fractions. Subsequently, peptides were combined into six fractions and dried by vacuum centrifugation. Peptides were first subjected to a nanospray ionization source and then tandem mass spectrometry (MS/MS) in a Q ExactiveTM Plus (Thermo Fisher Scientific, Waltham, MA, USA) coupled online to the UPLC. Data were obtained by searching through the human UniProt database for identified peptides assembled as proteins. The resulting MS/MS data were processed by the Maxquant search engine (v.1.5.2.8) and analyzed.

Western blotting

Proteins from KYSE150 cells treated with or without benzydamine were extracted using RIPA lysis buffer (Solarbio, Beijing, China, #R0020) and quantified using a bicinchoninic acid (BCA) assay kit (Beyotime, Shanghai, China, #P0011-1, #P0011-2) according to the manufacturer's protocol. Equal amounts of protein were prepared according to protein concentration and separated by SDS-PAGE. Proteins were subsequently electrophoretically transferred onto polyvinylidene fluoride membranes. After blocking with 5 % bovine serum albumin (Solarbio, Beijing, #A8020) or skimmed milk for 60 min at 25 °C, membranes were incubated with specific primary antibodies at 4 °C. Subsequently, incubation with horseradish peroxidase (HRP)-conjugated secondary antibodies was performed for 2 h at 25 °C. Blots were visualized using the enhanced chemiluminescence (ECL) detection reagent (GE Healthcare, Little Chalfont, UK). Primary antibodies used were: anti-p-MCM2 (Ser41) (#ab109270, 1:50000, Abcam, Cambridge, England), anti-MCM2 (#ab108935, 1:1000, Rabbit monoclonal, Abcam, Cambridge, England), anti-p-Rb (Thr826) (#ab133446, 1:1000, Rabbit monoclonal, Abcam, Cambridge, England), anti-Rb (#ab181616, 1:2000,

Rabbit monoclonal, Abcam, Cambridge, England), anti-p-c-Myc (Ser62) (#13748, 1:1000, Rabbit monoclonal, Cell Signaling Technology, Danvers, MA, USA), anti-c-Myc (#9402, 1:1000, Polyclonal Rabbit, Cell Signaling Technology, Danvers, MA, USA), and GAPDH (60004-1-Ig, 1:20,000, Mouse monoclonal, Proteintech, Wuhan, China).

Cell cycle analysis

Cells (3×10^5 cells) were seeded in 60-mm plates and synchronized by serum starvation for 24 h. Cells were then treated with benzydamine (0, 2.5, 5, 10, or 20 μM) for 24 h or 48 h in 10 % serum-supplemented medium. For cell cycle analysis, cells were harvested and washed with phosphate buffered saline twice, fixed in 70 % ethanol (Tianjin Zhiyuan Chemical Reagent Co., Ltd, China), and stored at -20 °C for 24 h. Cells were stained with propidium iodide (Beyotime, Shanghai, China) for cell cycle assessment, followed by analysis using a BD FACSCalibur Flow Cytometer (BD Biosciences, San Jose, CA).

Kinase prediction, target prediction, and correlation analysis

Kinase prediction of benzydamine was carried out using iGPS1.0 (http://igps.biocuckoo.org/). The target prediction of benzydamine was carried out by Swiss target prediction (http://www.swisstargetprediction.ch/). Correlation analysis of CDK2 and MCM2 was performed using The Cancer Genome Atlas (TCGA) database (https://www.aclbi.com/static/index.html#/).

Computational modelling of CDK2 with benzydamine

To explore the binding and interaction of CDK2 with benzydamine, we performed in silico docking using the autodock software programs. First, we downloaded the CDK2 crystal structure from the PDB (ID: 1AQ1) and prepared it using the standard procedures of the Protein Preparation Wizard (autodock). Hydrogen atoms were added at a pH of 7, and all water molecules were removed. The drug benzydamine was prepared for docking by using the default parameters in the LigPrep program. Subsequently, the docking of benzydamine to CDK2

was achieved using the default parameters in the extra precision (XP) mode in the Glide program.

Pull-down assay using CNBr-Sepharose 4B beads

Benzydamine-Sepharose 4B beads and dimethyl sulfoxide (DMSO)-Sepharose 4B beads were provided by GE Healthcare Bio-Science (Uppsala, Sweden) and prepared according to the manufacturer's instructions. Cell lysates (500 μg), active CDK2 (200 ng), and 293F cell lysate (500 μg) were incubated with benzydamine-Sepharose 4B beads and DMSO-Sepharose 4B beads in 1× reaction buffer (50 mM Tris pH 7.5, 5 mM EDTA, 150 mM NaCl, 1 mM DTT, 0.01 % NP-40, 2 μg/mL bovine serum albumin) at 4 °C with gentle rotation overnight. Beads were washed thrice with washing buffer (50 mM Tris-HCl pH 7.5, 5 mM EDTA, 150 mM NaCl, 1 mM DTT, 0.2 mM PMSF, and 0.01 % NP-40) after incubation. CDK2 bands were analyzed by western blotting.

Protein purification

PET-28a-CDK2 and MCM2 plasmids (purchased from YouBio Biotechnology Company, Hunan, China) were transformed in *E. coli* and amplified. Following amplification, the cells were lysed using ultrasounds, and the proteins obtained were purified by nickel column adsorption and elution. CDK2 and MCM2 proteins were identified by western blotting and Coomassie blue staining.

In vitro kinase assay

In vitro kinase assays were performed according to the manufacturer's instructions. Human recombined MCM2 protein (1 μg), used as a substrate for CDK2, was mixed with active CDK2 (500 ng) and varying doses of benzydamine in a 25 μL reaction mixture, which was supplemented with 20 μM ATP and 1× kinase buffer (Cell Signaling Technology, Danvers, MA, USA), followed by incubation at 30 °C for 30 min. Reactions were then blocked by the addition of 5 μL 6× loading buffer, and proteins were analyzed by western blotting.

Lentivirus production and infection

KYSE150 and KYSE450 cell lines were transfected with short hairpin RNA (shCDK2). The shCDK2 plasmids were cloned into the plko.1 lentiviral expression vector. The CDK2 clones (#1F: 5'-CCTCAGAATCTGCTTATTAAC-3'; #2F: 5'-GCCCTCTGAACTTGCCTTAAA-3'□ were purchased from Sangon Biotech (Shanghai, China). Both the viral and packaging vectors were added to HEK293T cells (60–80 % confluence). After 4 h, cells were placed in fresh medium (DMEM). The lentiviral particles were collected at 24, 48, and 72 h and harvested by filtration using a 0.22 μm filter. KYSE150 and KYSE450 cells (60 % confluence) were infected with medium containing lentiviral particles and 8 μg/mL polybrene for 12 h. Cells were then re-incubated in fresh medium for 24 h. Subsequently, 1 μg/mL (KYSE450) or 2 μg/mL (KYSE150) puromycin was used for cell selection. The transduction efficiency was analyzed by western blotting. The cell proliferation and colony formation ability of knockdown cells were examined in

comparison with mock-transfected cells. KYSE450 and KYSE150 cells were transfected with short hairpin CDK2 (shCDK2) in a similar manner.

Patient-derived xenograft (PDX) mouse model

All research protocols used in this study were approved by the Research Ethics Committee of Zhengzhou University. ESCC tissues were obtained from the Linzhou Tumour HospitalHenan. The protocols for establishing a PDX mouse model have been previously described [15, 16]. For these experiments, 6- to 8-week-old severe combined immunodeficient (SCID) female mice were used. Tumor tissues from patients were subcutaneously implanted into the back of SCID mice. When the tumor mass reached an average volume of 100 mm^3, mice were randomly divided into three treatment groups (n = 8-10/group) as follows: (1) vehicle group (n = 10); (2) 5 mg/kg benzydamine (n = 10); (3) 50 mg/kg benzydamine hydrochloride (n = 10). Benzydamine hydrochloride was administered using a gavage once a day for 30 days. Body weight was monitored three times per week. The tumor volume of each mouse was measured twice a week. Tumor volume was calculated using the following formula: $V = LD \times (SD)^2/2$, where V is the tumor volume. When the average tumor volume reached 1.0 cm^3, mice were euthanized under anesthesia and tumors were extracted.

Immunohistochemical staining assay

Formalin-fixed tumor tissue sections were deparaffinized, hydrated, and cut into 4-μm sections for immunohistochemistry. Samples were baked in a constant-temperature oven at 65 °C, and citrate acid was used for antigen retrieval. All tumor tissue sections were blocked with 3 % H_2O_2 for 10 min in the dark. Slides were then hybridized using specific antibodies (Ki-67, 1:50,Abcam, Cambridge, England; p-$MCM2^{S41}$, 1:200, Abcam, Cambridge, England) for 16 h at 4 °C and then incubated with an HRP-conjugated goat anti-rabbit or mouse IgG antibody (ZSGB-BIO, Beijing, China) for 30 min. After DAB staining for 2 min, sectioned tissues were counterstained with hematoxylin (Baso, Zhuhai, Guangdong, China) for 1 min, dehydrated in a graded series of alcohol to xylene, and covered with glass coverslips. All slides were observed under a microscope and scanned using the Tissue Faxes (version 4.2). The Image-Pro Plus software (v. 6) was used for measuring positive cells.

Statistical analysis

One-way analysis of variance or the Student's *t*-test was used to compare significant differences; $p < 0.05$ was considered statistically significant. All quantitative results were expressed as the mean ± standard deviation or ± standard error, as indicated.

Results

Benzydamine suppressed anchorage-dependent and -independent growth of ESCC

To identify a novel drug against ESCC, we screened FDA-approved drugs by performing a cytotoxic assay on KYSE450 cells. Benzydamine, a NSAID, exhibited significant cytotoxic effects in KYSE450 cells (Fig. 1a, b, Supplementary table1). To test the cytotoxic effect of benzydamine on human ESCC, we treated three different cell lines, KYSE150, KYSE450, and normal esophageal epithelial cells (SHEE), with varying concentrations of benzydamine for 24 and 48 h. Our results indicated that the half maximal inhibitory concentration (IC_{50}) of benzydamine on KYSE150, KYSE450, and SHEE cells at 48 h was 42.3, 36.2, and 125.61 μM, respectively (Fig. 1c). Subsequently, we used different doses of benzydamine to examine its effects on the anchorage-dependent growth of KYSE150, KYSE450, and SHEE cells. We found that benzydamine inhibited the anchorage-dependent growth of KYSE150 and KYSE450 cells (Fig. 1d). We then verified the effect of benzydamine on the anchorage-independent growth of KYSE150 and KYSE450 cells using a soft agar assay. Our results demonstrated that benzydamine suppressed the anchorage-independent growth of ESCC cells in a dose-dependent manner (Fig. 1e). Plate clone formation assays of KYSE150 and KYSE450 cells also indicated that benzydamine-treated groups had fewer colony numbers than the control group (Fig. 1f).

Phosphorylation profiles revealed the anti-tumor mechanism of benzydamine

To explore the inhibitory mechanism of benzydamine on ESCC, we conducted phosphoproteomic analysis to comprehensively analyze the changes in the phosphorylation level of proteins after treatment with benzydamine. Phosphorylation changes upon treatment with benzydamine were analyzed following a precise standard (*t*-test *p*-value < 0.05, 1.5-fold change from baseline as the threshold). We identified a total of 3 496 proteins, of which 2 982 proteins were quantified. Among the differentially expressed proteins, 159 proteins were upregulated, whereas 363 proteins were downregulated. We also identified a total of 14069 phosphorylation sites, among which 8509 sites were quantified. Among these quantified phosphosites, 191 sites were upregulated, whereas 500 sites were downregulated in KYSE150 cells after treated with 20 μM benzydamine (Fig. 2a-b). We then mapped the quantified phosphosites to Kyoto Encyclopedia of Genes and Genomes (KEGG) pathway enrichment. We observed that the top five down regulated signaling pathways included RNA transport, DNA replication, spliceosome, ferroptosis, and protein processing in the endoplasmic reticulum. The phosphoproteomic data suggested that multiple phosphorylation sites that have been essentially related with “cancer driver” genes were down regulated in the DNA replication signaling pathway (Fig. 2c). For instance, we found that the MCM2 S41 phosphosite was obviously down regulated in both the DNA replication and cell cycle signaling pathways (Fig. 2d). This phosphorylation site is known to participate in the initiation of DNA synthesis and is reportedly required for entry into the S phase and for cell division. Our results suggested that the phosphorylation level of MCM2 S41 was evidently inhibited after benzydamine treatment (Fig. 2e). To explore the underlying mechanism of the anti-tumor effect of benzydamine, we performed kinase prediction and SwissTargetPrediction to identify the upstream kinases. We observed that CDK2 was the most promising molecular target of benzydamine. Additionally, Spearman’s correlation analysis of the expression of the CDK2 and MCM2 genes representing the CDK2/MCM2 signaling pathway also showed significant differences (p = 2.58e-14) (Fig. 2f).

Benzydamine-induced G1/S phase arrest and inhibited the DNA replication pathway

We found that treatment with benzydamine affected the cell cycle distribution in the KYSE150 and KYSE450 ESCC cell lines (Fig. 3a, b). More specifically, benzydamine caused a significant G1/S phase cell cycle arrest in KYSE150 and KYSE450 cells ($p < 0.05$). Additionally, immunofluorescent experiments suggested the colocalization between p-MCM2 (Ser41) and CDK2 and benzydamine decreaed the phosphorylation of $MCM2^{S41}$ in KYSE150 and KYSE450 cells. Based on the results obtained, we detected the phosphorylation and expression levels of proteins involved in the transition from G1 to S phase during the cell cycle (Fig. 3c, d). We found that compared with the DMSO vehicle control, benzydamine reduced the phosphorylation of $MCM2^{S41}$, c-Myc^{S62} and Rb^{T826} in ESCC cells in a dose-dependent manner (Fig. 3e, f).

Benzydamine bound directly to CDK2 and inhibited CDK2 activity

Based on the SwissTarget and kinase prediction analysis, we hypothesized that CDK2 might be the upstream regulator of benzydamine in ESCC. To investigate the possible mechanism involved in the benzydamine-CDK2 interaction, we downloaded the CDK2 kinase domain (PDB: 1AQ1) and docked it with benzydamine following the protocols in the autodock software programs [17]. According to the docking model, we found that benzydamine formed a hydrogen bond with the CDK2 aspartic acid at site 145, which is also known to be an ATP-binding site affecting kinase activity. This suggested that benzydamine might be competing with ATP for binding at the ATP-binding site of CDK2 (Fig. 4a). To further verify this result, we performed a pull-down assay *in vitro* and *in vivo*, by conjugating benzydamine with Sepharose 4B beads. We found that the recombinant CDK2 protein kinase bound with benzydamine-conjugated Sepharose 4B beads but not with Sepharose 4B beads alone (Fig. 4b). We then constructed mutant CDK2 (F80A, D145A, F146A, D145A+146A) and ectopically expressed these mutants in 293F cells. Pull-down assays using wild-type or mutant CDK2 proteins and conjugated Sepharose 4B beads revealed that the D145A CDK2 mutant exhibited the greatest reduction in the binding affinity to benzydamine (Fig. 4c), indicating that Asp145 site is essential for binding (Fig. 4c). We further performed an *in vivo* pull-down assay using KYSE150 and KYSE450 cell lysates, and our results suggested that benzydamine could also bind to CDK2 *in vivo* (Fig. 4d). Interestingly, we also determined that the binding of benzydamine to CDK2 was ATP-competitive. We observed that benzydamine competed with ATP for binding at the ATP-binding site of CDK2, Asp145 (Fig. 4e). And, sequence alignment of CDK2 phosphorylation consensus show highly evolutionarily conserved among multiple species suggesting that Asp145 was a functional phosphorylation site (Fig. S3). Next, we performed an *in vitro* kinase assay using an active recombinant CDK2 protein and MCM2 as a substrate, to verify whether CDK2 was the direct target of benzydamine. Our results suggested that the activity of CDK2 was strongly inhibited by treatment with benzydamine in a dose-dependent manner (Fig. 4f, g) and confirmed that benzydamine directly suppressed the activity of CDK2, resulting in inhibition of CDK2 phosphorylation of MCM2 on serine, especially on serine 41.

Knockdown of CDK2 decreased the sensitivity of ESCC cells to benzydamine

TCGA analysis of CDK2 suggested that CDK2 is highly expressed in EC (Fig. 5a). To further explore the function of CDK2 in ESCC tumor growth, we performed experiments after knocking-down CDK2. After transfecting KYSE150 and KYSE450 cells with *sh*-CDK2, the total protein level of CDK2 was measured to verify the efficiency of transfection and CDK2 knockdown also decreased the phosphorylation of related downstream biomarkers (Fig. 5b). We also found that the CDK2 knockdown suppressed the proliferation of KYSE150 and KYSE450 cells (Fig. 5c). Moreover, we noticed that the colony formation ability of these cells was also inhibited after CDK2 was knocked-down (Fig. 5d, e). effect of the CDK2 knockdown was also detected in cell cycle distribution (Fig. 5f, g). Our results suggested that knocking-down CDK2 induced a G1/S phase arrest in KYSE150 and KYSE450 cells. Benzydamine was shown to specifically target CDK2; therefore, we further investigated whether knockdown of CDK2 could affect the sensitivity of ESCC cells to benzydamine. We observed that following CDK2 knockdown, treatment with benzydamine had no obvious effect on the anchorage-dependent growth compared with that in mock-transfected cells. Moreover, the benzydamine-induced inhibition of both the proliferation of ESCC cells was weakened by the CDK2 knockdown (Fig. 5h).

Benzydamine suppressed patient-derived esophageal xenograft tumor growth *in vivo*

We used the PDX model to evaluate the anti-tumor activity of benzydamine *in vivo*. Tumor tissue from patients was implanted into the backs of SCID mice. Mice were administered benzydamine hydrochloride (5 and 50 mg/kg) or vehicle. We found that benzydamine suppressed the volume of tumor growth relative to the vehicle-treated group, while, the average body weight was not obviously different between different groups (Fig. 6a, b, Fig. S4). The mice were euthanized, and the weight of tumor tissues was measured; we observed that an increase in tumor weight was inhibited in mice treated with benzydamine (Fig. 6c).

In addition, we also observed that benzydamine-treated mice did not exhibit an obvious loss of body weight compared with the vehicle-treated group. We then verified the findings of the phosphoproteomic profile at the tissue level using immunohistochemistry. Our results demonstrated that benzydamine decreased the expression of Ki67 and the phosphorylation level of $MCM2^{S41}$ (Fig. 6d).

Discussion

The incidence and mortality of EC was reportedly ranked in the seventh and sixth place, respectively, among all cancers in 2020 [18]. Thus, there is an urgent need for the identification of new inhibitors for effective targeted therapies. Recently, the application of FDA-approved drugs has become a new approach for chemoprevention [8]. These agents have the potential to reduce the onset of cancer and its relapse after treatment by inhibiting signaling molecules of great importance in carcinogenic events [19]. In this study, we showed that the NSAID benzydamine significantly inhibited the proliferation and colony formation of ESCC cells *in vitro*, as well as the tumor growth of patient-derived esophageal xenografts of ESCC *in vivo* (Fig. 1 and 6). We identified a novel drug with chemopreventive potential, especially against CDK2-dependent cancers.

We performed mass spectrometry to explore the systemic pharmacology of the inhibitory effect of benzydamine on ESCC cells. Analysis of the phosphoproteome and KEGG enrichment suggested that benzydamine significantly downregulated the DNA replication signaling pathway, which is essential for cell cycle and genome stability [20]. Additionally, analysis of differentially-phosphorylated sites indicated that the phosphorylation levels of $MCM2^{S41}$, Rb^{T826}, and c-Myc^{S62} were decreased. Combined with kinase prediction, Swiss target prediction, and *in vitro* assays, CDK2 was identified as the potential target of benzydamine (Fig. 2, 4).

CDK2 belongs to the family of cyclin-dependent kinase complexes and plays a key role in the cell division cycle [21]. In particular, CDK2 is known to be activated by binding to cyclin E1 or E2, and the activity of both cyclin A2 and CDK2 is critically related to tumor growth in many cancer types [14]. The cyclin E-CDK2 complex acts as a master regulator of the progression from the late G1 phase to the S phase [13, 22], which is essential for eukaryotic cell proliferation and its mis-regulation has been shown to enhance oncogenesis [23]. Inhibition of cyclin E-CDK2 leads to a G1/S arrest, blocking cell cycle progression [13, 24]. Therefore, we also investigated the potential inhibitory mechanisms of benzydamine on the growth of EC. We found that benzydamine induced a G1/S arrest in ESCC cells in a dose-dependent manner by inhibiting the activity of CDK2 (Fig. 3).

Moreover, CDK2 has been shown to specifically phosphorylate MCM2, Rb, and c-Myc. During the G1 to S transition, cyclin E-CDK2 was found to phosphorylate MCM2 at Ser 41 to initiate DNA synthesis [25, 26]. Meanwhile, this complex has also been reported to catalyze the hyper-phosphorylation of Rb at Thr 826, resulting in the promotion of tumor growth [27]. Additionally, cyclin E/CDK2 is known to phosphorylate c-Myc at Ser 62 and the phosphorylation can increase the biological activity of Myc, which regulating cell cycle and tumor initiation [28, 29]. Our results indicated that benzydamine decreased the phosphorylation of $MCM2^{S41}$, RB^{T826}, and c-Myc^{S62} by binding to CDK2 and inhibiting its activity, which has been critically related to tumor growth in many cancer types. To our knowledge, this is the first study elucidating the anti-tumor effect of benzydamine. In addition, we explored whether the inhibitory effect of benzydamine on ESCC cells depended on the expression of CDK2. To this end, we established cells expressing *sh*-CDK2. We found that knocking-down CDK2 restrained the growth and colony formation of ESCC cells. Furthermore, ESCC cells expressing *sh*-CDK2 were less sensitive to benzydamine than cells expressing *sh*-control (Fig. 5). Therefore, we assumed that CDK2 is the major target protein of benzydamine in EC cells.

A computational modelling system could identify the critical interacting residues between target proteins and natural compounds [30, 31]. By utilizing computational modelling, we simulated the binding model of benzydamine to CDK2. We computationally predicted that benzydamine possesses a series of binding orientations in the ATP-binding site of CDK2 (Fig. 4a). In addition, an *in vitro* and *in vivo* binding assay suggested that the Asp145 residue of CDK2 is critically essential for binding, affecting the kinase activity (Fig. 4b-e).

PDX models provide a series of advantages over human cell line xenograft models for the evaluation of preclinical therapies and prediction of responsiveness to anti-cancer treatments because they retain more

genetic characteristics of the tumor specimens of patients [32-34]. In this study, we constructed PDX models in immunodeficient mice by subcutaneously inoculating them with tumor tissues from an ESCC patient [35]. We found that benzydamine suppressed tumor growth of ESCC and PDX tumors in mice by attenuating the phosphorylation of MCM2 at serine 41. Additionally, the expression of Ki67, a proliferation marker [36], was also shown to be decreased in tumor tissues after treatment with benzydamine (Fig. 6). These findings indicated that benzydamine could suppress the tumor growth of ESCC *in vivo* by targeting the CDK2/MCM2 signaling pathway.

Benzydamine has been used to prevent postoperative sore throat [37], to treat oral mucositis, and for pain relief in patients with cancer receiving chemotherapy, radiotherapy, or both [38]. However, beyond its original use, this is the first study to establish the anti-tumor activity of benzydamine in EC through the targeting of CDK2. Based on the similarity of the ATP-binding pocket and interaction between the CDK proteins, we assumed that a number of specific cancers could benefit from the combined inhibition of CDK2 with other CDKs [39]. Thus, the inhibition of CDK2 could be combined with various modalities of treatment, such as chemotherapy, radiotherapy, and targeted inhibitors, to reduce the proliferation of tumor cells [13, 40, 41].

Overall, our study suggested that benzydamine could inhibit the progression of ESCC tumors, both *in vitro* and *in vivo*, by suppressing the DNA replication signaling pathway by targeting CDK2 (Fig. 7). Thus, this study could provide useful information for the clinical application of benzydamine in ESCC chemoprevention and combination therapy.

Conclusions

In summary, our results revealed a novel drug against ESCC. Benzydamine directly binds with CDK2 and inhibits its kinase activity, down-regulating the phosphorylation levels of MCM2, c-Myc and Rb, induces cell cycle arrest, and exerts the inhibitory effect on ESCC proliferation *in vivo* and *in vitro*. This study provides a new strategy for cancer chemoprevention of esophageal squamous cell carcinoma.

Abbreviations

APS, Ammonium persulfate; BSA, bovine serum albumin; CDK2, Cyclin-dependent kinase 2; DAPI, 4',6-diamidino-2-phenylindole; DMEM; Dulbecco's Modified Eagle's medium; DMSO, Dimethyl sulfoxide; ESCC, Oesophageal squamous cell carcinoma; FBS, foetal bovine serum; FDA, Food and Drug Administration; HRP, horseradish peroxidase; KEGG, Kyoto Encyclopedia of Genes and Genomes; MCM2, Minichromosome maintenance protein; PDX, Patient-derived Xenograft; TCGA, The Cancer Genome Atlas.

Declarations

Ethics approval and consent to participate

This study was approved by the Research Ethics Committee of Zhengzhou University. Written informed consent was provided by all patients for the use of the tissue samples.

Consent for publication

All authors have given their consent for the publication of this article.

Availability of data and materials

The raw data supporting the conclusions of this article will be made available by the authors, without undue reservation, to any qualifified researcher.

Competing interests

All authors declare that they have no competing interests.

Findings

This work was supported by the National Natural Science Foundations of China (No. 81872335), National Natural Science Youth Foundation (No. 426 81902486), the Natural Science Foundation of Henan (No. 161100510300), National Science & Technology Major Project Key New Drug Creation and Manufacturing Program, China (No. 2018ZX09711002), the Science and Technology Project of Henan Province (No. 212102310187).

Authors'contributions

YBZ performed the conceptualization, data curation and writing - original draft. XYH performed the software and validation. YNJ contributed the methodology, writing - review & editing, funding acquisition. ZTW performed the formal analysis. YY contributed the methodology. WJW collected the resources. CYZ, JCL, YPG performed the validation. XHC, ZCL contributed the investigation. JMZ perfomed the data curation. ZGD contributed the visualization and supervision. KDL contributed the supervision, project administration and funding acquisition.

Acknowledgements

Not applicable.

Author details

[1] The Pathophysiology Department, The School of Basic Medical Sciences, Zhengzhou University, Zhengzhou 450000, China.

[2] China-US (Henan) Hormel Cancer Institute, Zhengzhou 450000, China.

[3] State Key Laboratory of Esophageal Cancer Prevention and Treatment, Zhengzhou 450000, Henan, China.

[4] Provincial Cooperative Innovation Center for Cancer Chemoprevention, Zhengzhou University 450000, Zhengzhou, Henan, China.

[5] Cancer Chemoprevention International Collaboration Laboratory, Zhengzhou 450000, Henan, China

[6] Oncology Department, The Tumor Hospital of Linzhou City, Linzhou 456500, Henan, China

References

1. References.
2. Z Y. X W, X G, Y L, J M, F T, et al. Liquid biopsy for esophageal cancer: Is detection of circulating cell-free DNA as a biomarker feasible? Cancer communications (London, England). 2020. 10.1002/cac2.12118.
3. Cc A, Wq MA. W. Epidemiology of Esophageal Squamous Cell Carcinoma. Gastroenterology. 2018;154(2):360–73. 10.1053/j.gastro.2017.08.023.
4. Ym Y, P H, Ww X, Qy H. B L. Advances in targeted therapy for esophageal cancer. Signal transduction targeted therapy. 2020;5(1):229. 10.1038/s41392-020-00323-3.
5. di Pietro M, Mi C, Rc F. Endoscopic Management of Early Adenocarcinoma and Squamous Cell Carcinoma of the Esophagus: Screening, Diagnosis, and Therapy. Gastroenterology. 2018;154(2):421–36. 10.1053/j.gastro.2017.07.041.
6. Reichenbach ZW, Murray MG, Saxena R, Farkas D, Karassik EG, Klochkova A, et al. Clinical and translational advances in esophageal squamous cell carcinoma. Adv Cancer Res. 2019;144:95–135. 10.1016/bs.acr.2019.05.004.
7. Surh YJ. Cancer chemoprevention with dietary phytochemicals. Nat Rev Cancer. 2003;3(10):768–80. 10.1038/nrc1189.
8. Desai P, Thumma NJ, Wagh PR, Zhan S, Ann D, Wang J, et al. Cancer Chemoprevention Using Nanotechnology-Based Approaches. Front Pharmacol. 2020;11:323. 10.3389/fphar.2020.00323.
9. Mohammed A, Fox JT, Miller MS. Cancer Chemoprevention: Preclinical In Vivo Alternate Dosing Strategies to Reduce Drug Toxicities. Toxicol Sci. 2019;170(2):251–9. 10.1093/toxsci/kfz104.
10. Ranjan A, Ramachandran S, Gupta N, Kaushik I, Wright S, Srivastava S, et al. Role of Phytochemicals in Cancer Prevention. Int J Mol Sci. 2019;20(20). 10.3390/ijms20204981.
11. Chen CY, Kuo CJ, Lee YW, Lam F, Tam KW. Benzydamine hydrochloride on postoperative sore throat: a meta-analysis of randomized controlled trials. Can J Anaesth. 2014;61(3):220–8. 10.1007/s12630-013-0080-y.
12. Tetsu O, Mccormick F. Proliferation of cancer cells despite CDK2 inhibition. Cancer Cell. 2003;3(3):233–45. 10.1016/s1535-6108(03)00053 – 9.

13. Au-Yeung G, Lang F, Azar WJ, Mitchell C, Jarman KE, Lackovic K, et al. Selective Targeting of Cyclin E1-Amplified High-Grade Serous Ovarian Cancer by Cyclin-Dependent Kinase 2 and AKT Inhibition. Clin Cancer Res. 2017;23(7):1862–74. 10.1158/1078 – 0432.CCR-16-0620.
14. At ST, N A, W PEL, Ce T. C, et al. Targeting CDK2 in cancer: challenges and opportunities for therapy. Drug Discov Today. 2020;25(2):406–13. 10.1016/j.drudis.2019.12.001.
15. Ec ST, W C, Cyclin-Dependent TSW. Kinase 2 Inhibitors in Cancer Therapy: An Update. J Med Chem. 2019;62(9):4233–51. 10.1021/acs.jmedchem.8b01469.
16. Jiang Y, Wu Q, Yang X, Zhao J, Jin Y, Li K, et al. A method for establishing a patient-derived xenograft model to explore new therapeutic strategies for esophageal squamous cell carcinoma. Oncol Rep. 2016;35(2):785–92. 10.3892/or.2015.4459.
17. Jin G, Yan M, Liu K, Yao K, Chen H, Zhang C, et al. Discovery of a novel dual-target inhibitor against RSK1 and MSK2 to suppress growth of human colon cancer. Oncogene. 2020;39(43):6733–46. 10.1038/s41388-020-01467-w.
18. ©. 1997 Nature Publishing Group http://www.nature.com/nsmb.
19. Global Cancer Statistics. 2020: GLOBOCAN Estimates of Incidence and Mortality Worldwide for 36 Cancers in 185 Countries.
20. Raimundo L, Ramos H, Loureiro JB, Calheiros J, Saraiva L. BRCA1/P53: Two strengths in cancer chemoprevention. Biochim Biophys Acta Rev Cancer. 2020;1873(1):188339. 10.1016/j.bbcan.2020.188339.
21. B P MM. T V, A A, P P. Homologous recombination and Mus81 promote replication completion in response to replication fork blockage. Embo Rep. 2020;21(7):e49367. 10.15252/embr.201949367.
22. Rm G. Cdk1 and Cdk2 complexes (cyclin dependent kinases) in apoptosis: a role beyond the cell cycle. Cancer Lett. 2005;217(2):129–38. 10.1016/j.canlet.2004.08.005.
23. Hc H, Be C. Cyclin E in normal and neoplastic cell cycles. Oncogene. 2005;24(17):2776–86. 10.1038/sj.onc.1208613.
24. Bertoli C, Skotheim JM, de Bruin RA. Control of cell cycle transcription during G1 and S phases. Nat Rev Mol Cell Biol. 2013;14(8):518–28. 10.1038/nrm3629.
25. Pagano M, Pepperkok R, Lukas J, Baldin V, Ansorge W, Bartek J, et al. Regulation of the cell cycle by the cdk2 protein kinase in cultured human fibroblasts. J Cell Biol. 1993;121(1):101–11. 10.1083/jcb.121.1.101.
26. Tsuji T, Ficarro SB, Jiang W. Essential role of phosphorylation of MCM2 by Cdc7/Dbf4 in the initiation of DNA replication in mammalian cells. Mol Biol Cell. 2006;17(10):4459–72. 10.1091/mbc.e06-03-0241.
27. Poon RY. Cell Cycle Control: A System of Interlinking Oscillators. Methods Mol Biol 2016;1342:3–19. 10.1007/978-1-4939-2957-3$41.
28. Harbour JW, Luo RX, Dei SA, Postigo AA, Dean DC. Cdk phosphorylation triggers sequential intramolecular interactions that progressively block Rb functions as cells move through G1. Cell.

1999;98(6):859–69. 10.1016/s0092-8674(00)81519-6.

29. Lg PH. L. Tipping the balance: Cdk2 enables Myc to suppress senescence. Cancer Res. 2010;70(17):6687–91. 10.1158/0008-5472.CAN-10-1383.
30. Hydbring P, Castell A, Larsson L. MYC Modulation around the CDK2/p27/SKP2 Axis. Genes-Basel. 2017;8(7):174.
31. Musyoka TM, Kanzi AM, Lobb KA, Tastan B. Structure Based Docking and Molecular Dynamic Studies of Plasmodial Cysteine Proteases against a South African Natural Compound and its Analogs. Sci Rep. 2016;6:23690. 10.1038/srep23690.
32. Grover S, Dhanjal JK, Goyal S, Grover A, Sundar D. Computational identification of novel natural inhibitors of glucagon receptor for checking type II diabetes mellitus. Bmc Bioinformatics. 2014;15(Suppl 16):13. 10.1186/1471-2105-15-S16-S13. Suppl 16) .
33. Pl G, Al M, Kj Y. Patient-Derived Xenograft Models of Pancreatic Cancer: Overview and Comparison with Other Types of Models. Cancers. 2020;12(5). 10.3390/cancers12051327.
34. Mj SKSDAB, U P. K, S S. From Cancer to Immune-Mediated Diseases and Tolerance Induction: Lessons Learned From Immune Oncology and Classical Anti-cancer Treatment. Front Immunol. 2020;11:1423. 10.3389/fimmu.2020.01423.
35. Hidalgo M, Amant F, Biankin AV, Budinská E, Byrne AT, Caldas C, et al. Patient-derived xenograft models: an emerging platform for translational cancer research. Cancer Discov. 2014;4(9):998–1013. 10.1158/2159–8290.CD-14-0001.
36. Yoshida GJ. Applications of patient-derived tumor xenograft models and tumor organoids. J Hematol Oncol. 2020;13(1):4. 10.1186/s13045-019-0829-z.
37. Dowsett M, Nielsen TO, A'Hern R, Bartlett J, Coombes RC, Cuzick J, et al. Assessment of Ki67 in breast cancer: recommendations from the International Ki67 in Breast Cancer working group. J Natl Cancer Inst. 2011;103(22):1656–64. 10.1093/jnci/djr393.
38. Kuriyama A, Maeda H. Topical benzydamine for preventing postoperative sore throat. A reply. Anaesthesia. 2018;73(10):1298. 10.1111/anae.14438.
39. Worthington HV, Clarkson JE, Eden OB. Interventions for preventing oral mucositis for patients with cancer receiving treatment. Cochrane Database Syst Rev. 2006(2):CD000978. 10.1002/14651858.CD000978.pub2.
40. Knockaert M, Greengard P, Meijer L. Pharmacological inhibitors of cyclin-dependent kinases. Trends Pharmacol Sci. 2002;23(9):417–25. 10.1016/s0165-6147(02)02071-0.
41. Wang J, Yang T, Xu G, Liu H, Ren C, Xie W, et al. Cyclin-Dependent Kinase 2 Promotes Tumor Proliferation and Induces Radio Resistance in Glioblastoma. Transl Oncol. 2016;9(6):548–56. 10.1016/j.tranon.2016.08.007.
42. Beale G, Haagensen EJ, Thomas HD, Wang LZ, Revill CH, Payne SL, et al. Combined PI3K and CDK2 inhibition induces cell death and enhances in vivo antitumour activity in colorectal cancer. Br J Cancer. 2016;115(6):682–90. 10.1038/bjc.2016.238.

Figures

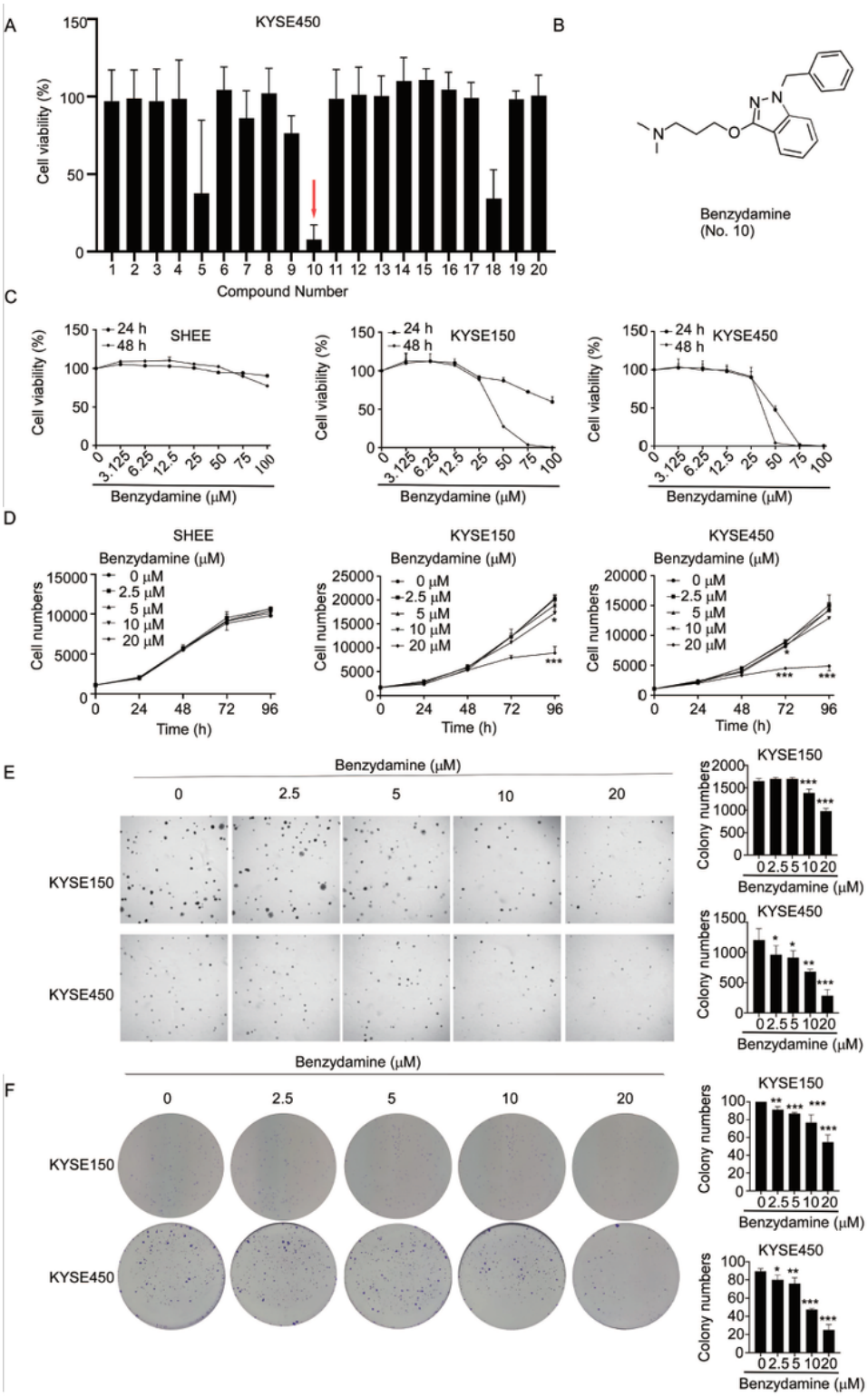

Figure 1

Benzydamine suppresses the anchorage-independent and -independent growth of ESCC cells (a) Effect of 50 FDA-approved drugs on cell proliferation. KYSE450 cells were treated with these drugs (50 μM) for 48 h and the cell survival rate was calculated. (No. 1-20) (b) Chemical structure of benzydamine. (c)

KYSE150, KYSE450, and SHEE cells treated with benzydamine for 24 and 48 h. Cell viability in the cytotoxicity assay was measured using the IN Cell Analyzer 6000 software. (d) Effect of benzydamine on the proliferation of SHEE cells and ESCC cells treated with varying doses of benzydamine for 24, 48, 72, and 96 h. (e) Soft agar assay of ESCC cells treated with benzydamine for 2 wk. Colony numbers were counted using the IN Cell Analyzer 6000 and Image J software. Quantitative analysis is on the right. (f) Clone formation assay and quantitative analysis conducted on KYSE150 and KYSE450 cells for 1 wk. Cells were treated with varying concentrations of benzydamine and then stained with crystal violet dye. The data in (d-f) were derived from three independent experiments and are presented as mean ± SD. Asterisks (*, **, ***) indicate a significant decrease ($p < 0.05$, $p < 0.01$, $p < 0.001$, respectively) by one-way ANOVA followed by multiple-comparison tests. Similar results were obtained in three independent experiments.

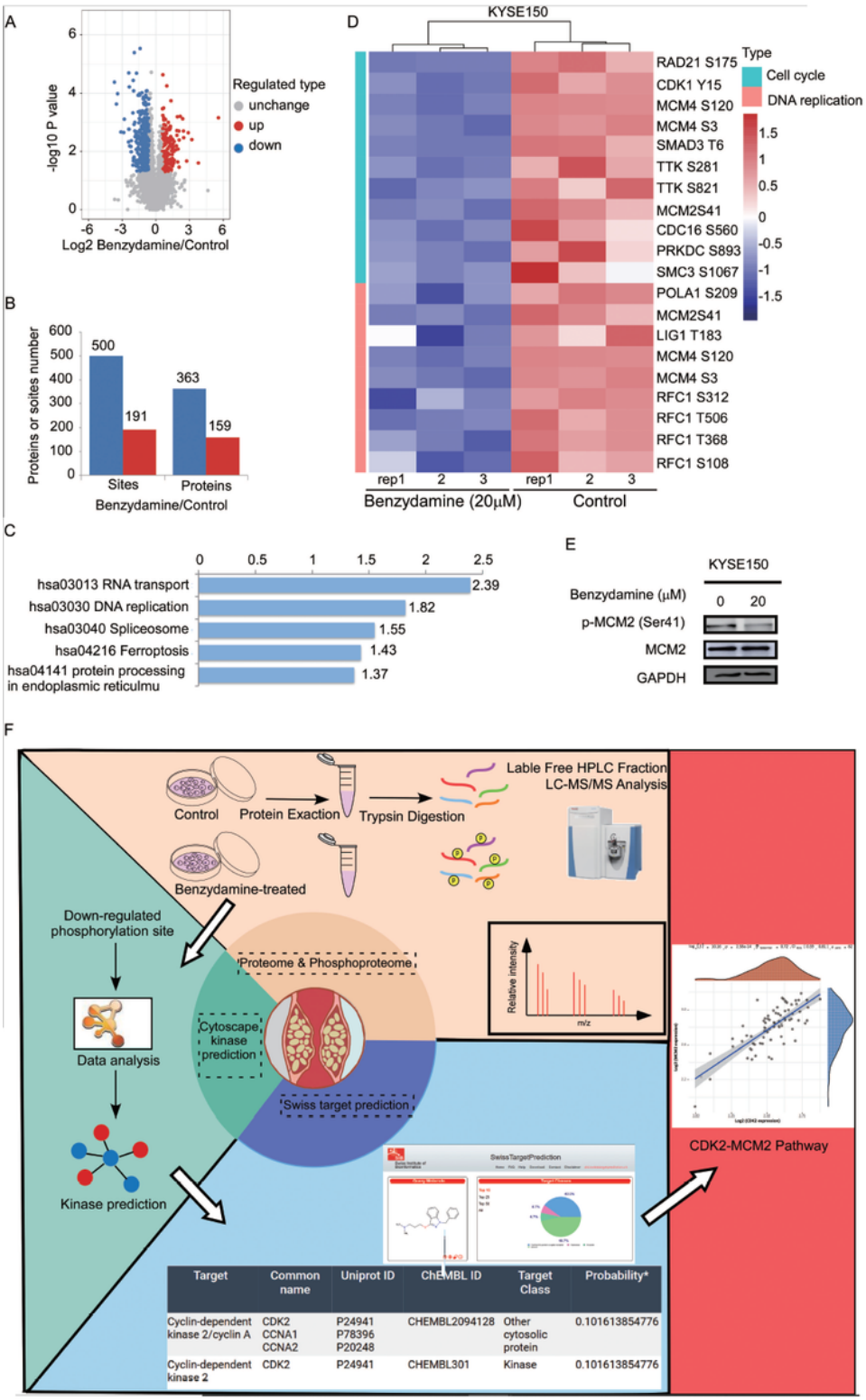

Figure 2

Phosphorylation profiles reveal the anti-tumor mechanism of benzydamine (a) Volcano plot of differentially-expressed phosphorylation sites. Blue dots represent downregulated sites, whereas red dots represent upregulated sites. (b) Quantification of differentially-expressed proteins and modified phosphorylation sites. (c) KEGG enrichment of downregulated phosphorylation sites (top five pathways). (d) Significantly changed phosphorylation sites involved in DNA replication and cell cycle signaling

pathways are shown in heatmap. (e) Phosphorylation and expression levels were assessed by western blotting. KYSE150 cells were treated with or without benzydamine for 24 h. (f) The exploration pipeline for analysis of multi-omics data and prediction of upstream protein kinases. The LC-MS/MS search and database research were first constructed for the proteome and phosphoproteome analyses. Kinase and Swiss target prediction were subsequently employed to predict upstream kinases. Spearman's correlation analysis of the expression of CDK2 and MCM2 genes. Datasets used were comprised of mRNA-seq data from TCGA tumors (see TCGA Data Portal at https://tcga-data.nci.nih.gov/tcga/.) Quantified protein and phosphorylation sites were subjected to the following criteria ($p < 0.05$, fold change > 1.5).

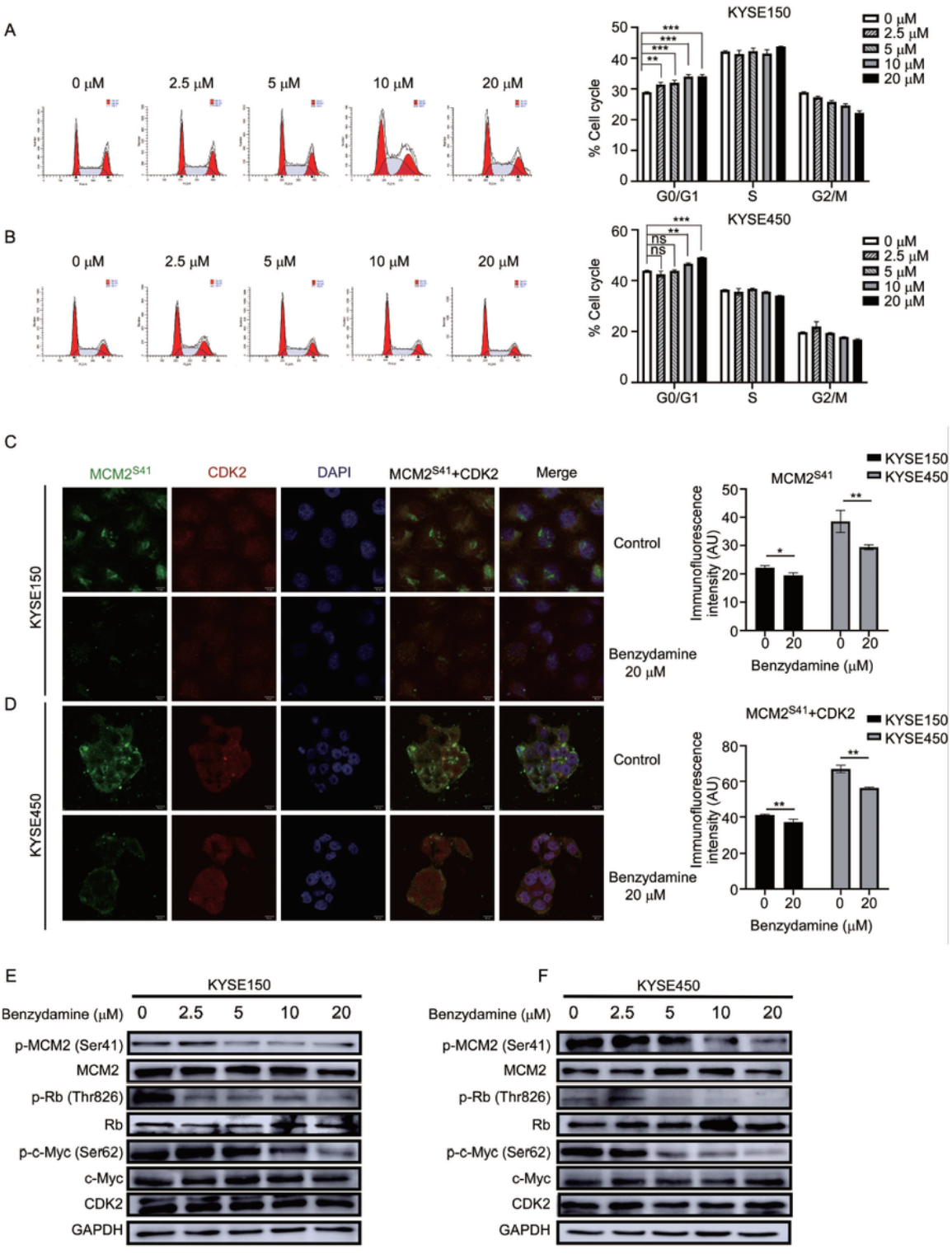

Figure 3

Benzydamine induces G1/S phase arrest and inhibits the DNA replication pathway (a, b) The effects of benzydamine on cell cycle phase were demonstrated using KYSE150 and KYSE450 ESCC cell lines. Cells were treated with varying concentrations of benzydamine (0, 2.5, 5, 10, and 20 μM) and incubated for 24 h (KYSE150) or 48 h (KYSE450) for cell cycle analysis by flow cytometry. Bar graph indicates the distribution of cell cycle in KYSE150 and KYSE450 ESCC cell lines. (c, d) Immunofluorescence staining of

KYSE150 and KYSE450 cells with or without benzydamine treatment for 24 h. Cells were stained with DAPI (blue in), anti-CDK2 (red) and anti-MCM2S41 (green). Double immunofluorescence indicated colocalization between MCM2S41 and CDK2. Scale bars, 10 μm. (e, f) Effect of benzydamine on the expression of biomarkers associated with the G1 to S phase transition during the cell cycle. KYSE150 and KYSE450 cells were treated with 0, 2.5, 5, 10, or 20 μM benzydamine and incubated for 24 h before detection. For the data in (a-d), asterisks (**$p < 0.01$, ***$p < 0.001$) indicate a significant difference between untreated control and benzydamine-treated KYSE150 and KYSE450 cells. Data are expressed as mean ± SD by one way ANOVA followed by multiple comparisons.

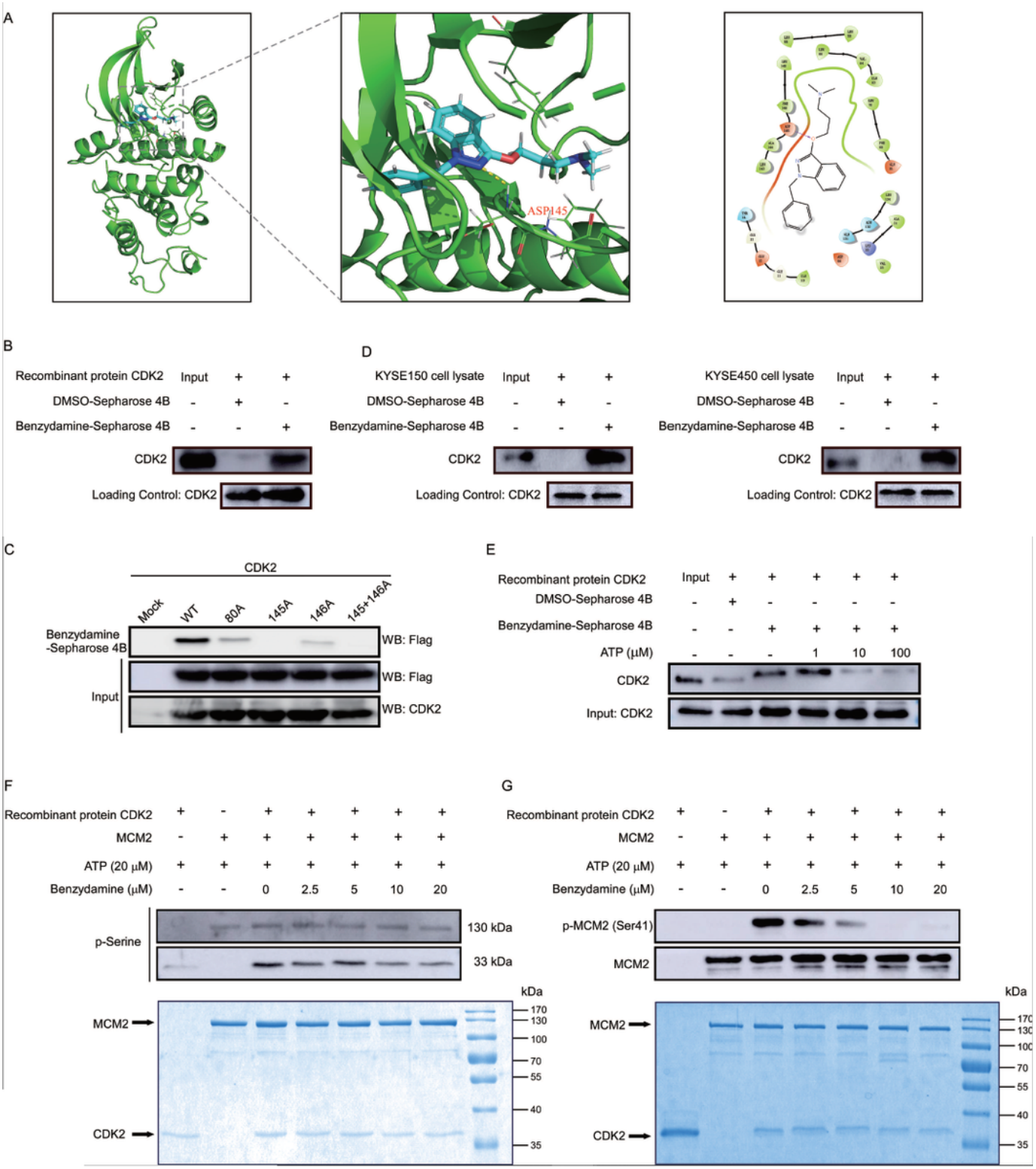

Figure 4

Benzydamine can directly bind to CDK2 and inhibit CDK2 activity (a) Modelling of benzydamine binding to CDK2 at the ATP-binding site. (b, d) Active CDK2 (200 ng) and cell lysates of KYSE150 and KYSE450 were incubated with benzydamine-conjugated Sepharose 4B beads or with Sepharose 4B beads alone. Pull-down proteins were analyzed by western blotting. (c) Recombinant proteins or cells ectopically expressing CDK2 (WT, mutant F80A, D145A, F146A, D145A+146A) were incubated with benzydamine-

conjugated Sepharose 4B beads or with Sepharose 4B beads alone. Pull-down proteins were analyzed by western blotting. (e) The specificity of the binding of benzydamine to active CDK2 in the presence of ATP was evaluated. (f, g) Active CDK2 (500 ng) and various doses of benzydamine were incubated with MCM2 (1 μg) as a substrate at 30 °C for 30 min. The phosphorylation of MCM2 (Serine, Ser 41) was detected by western blotting. Our results revealed that benzydamine inhibited the activity of the CDK2 kinase in vitro. CDK2 and MCM2 proteins were detected by western blotting and Coomassie blue staining (The bottom picture).

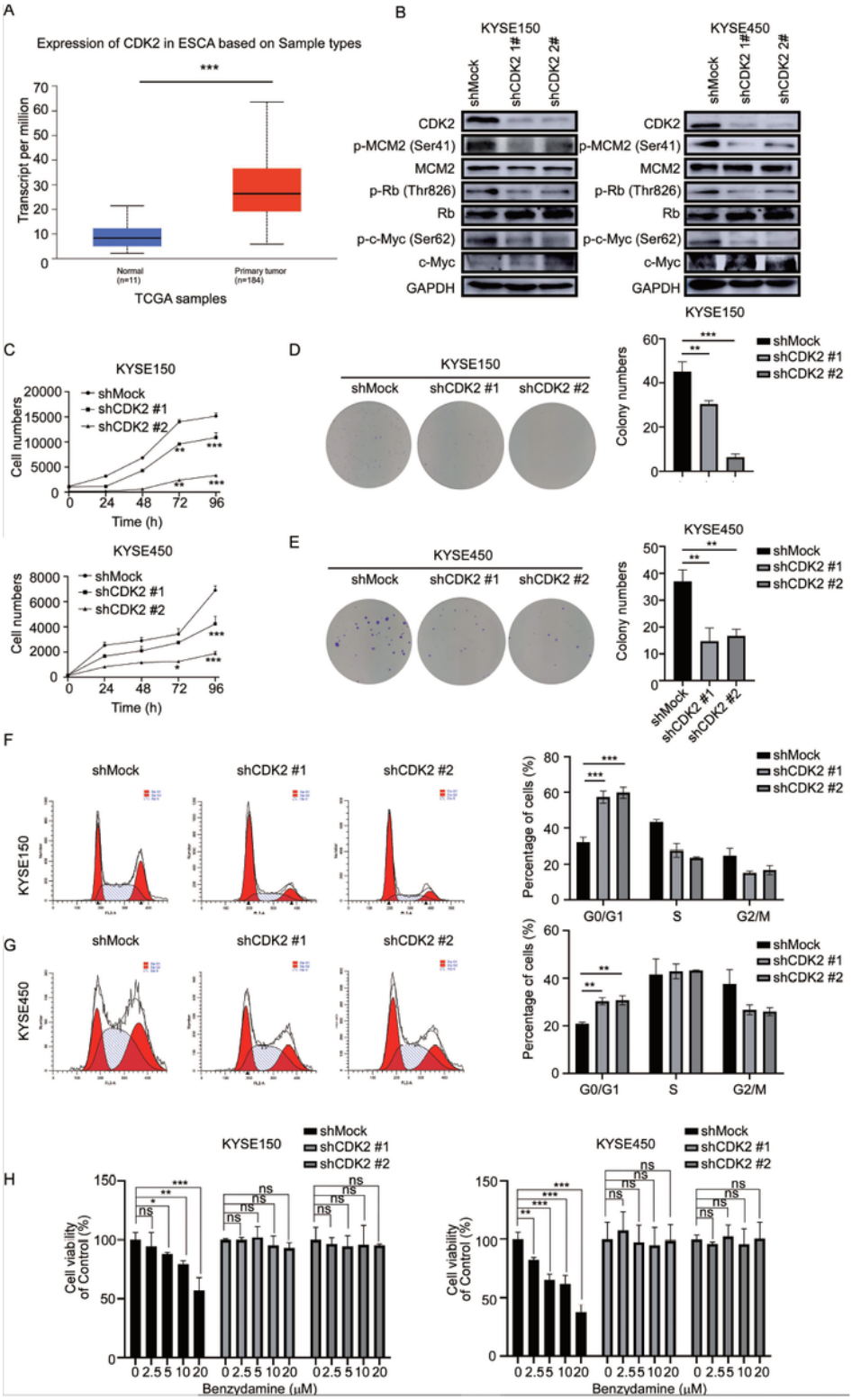

Figure 5

Knockdown of CDK2 restrains the anchorage-dependent and -independent growth of ESCC cells and decreases the sensitivity of ESCC cells to benzydamine (a) CDK2 was significantly expressed in EC tumor tissues compared with that in normal tissues as revealed by analyzing the available data from TCGA database (p=1.76390000050652E-07). (b) Knockdown of CDK2 expression or targets downstream of CDK2 in KYSE150 and KYSE450 ESCC cell lines. Similar results were obtained in three independent experiments. (c-e) Knocking-down the expression of CDK2 in KYSE150 and KYSE450 cells reduced the proliferation and colony formation ability of ESCC cells. Proliferation assay (c), Plate cloning assay (d, e). (f, g) Knocking-down the expression of CDK2 in KYSE150 and KYSE450 cells induced a G1/S phase arrest. (h) Proliferation of KYSE150 and KYSE450 cells transfected with shmock or shCDK2, with or without treatment with varying doses of benzydamine (0, 2.5, 5, 10, or 20 μM). Cell numbers were measured using the IN Cell Analyzer 6000 software. For (c-h), data are shown as the mean ± SD of triplicate values obtained from three independent experiments. Asterisks (*, **, ***) indicate a significant decrease ($p < 0.05$, $p < 0.01$, $p < 0.001$, respectively) by one-way ANOVA followed by multiple-comparison tests.

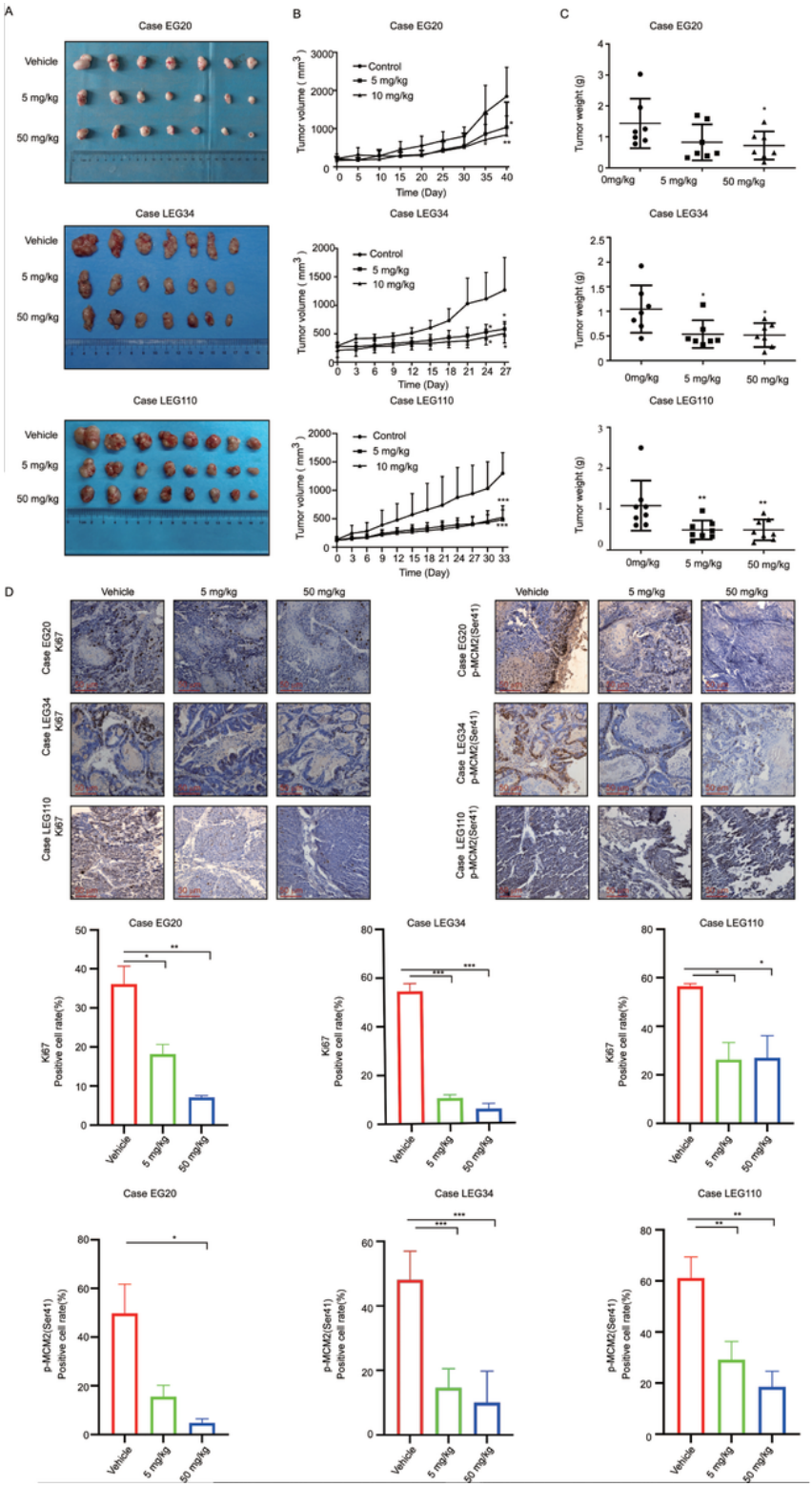

Figure 6

Benzydamine suppresses patient-derived esophageal xenograft tumor growth in vivo (a, b, c) Effect of benzydamine on tumor growth. Vehicle or benzydamine hydrochloride (5 or 50 mg/kg) was administered by gavage. Benzydamine significantly suppressed the tumor growth of cases EG20, LEG34, and LEG110. Plotted tumor volume and tumor weight. (d) Immunohistochemistry analysis of Ki67, p-MCM2 S41 stained with DAB in cases EG20, LEG34, and LEG110 after administration of benzydamine. The positive

cell rate was evaluated by Histo Quest-shortcut software. All data are shown as the mean ± SD. Asterisks (*, **, ***) indicate a significant decrease ($p < 0.05$, $p < 0.01$, $p < 0.001$, respectively) by one-way ANOVA followed by multiple-comparison tests.

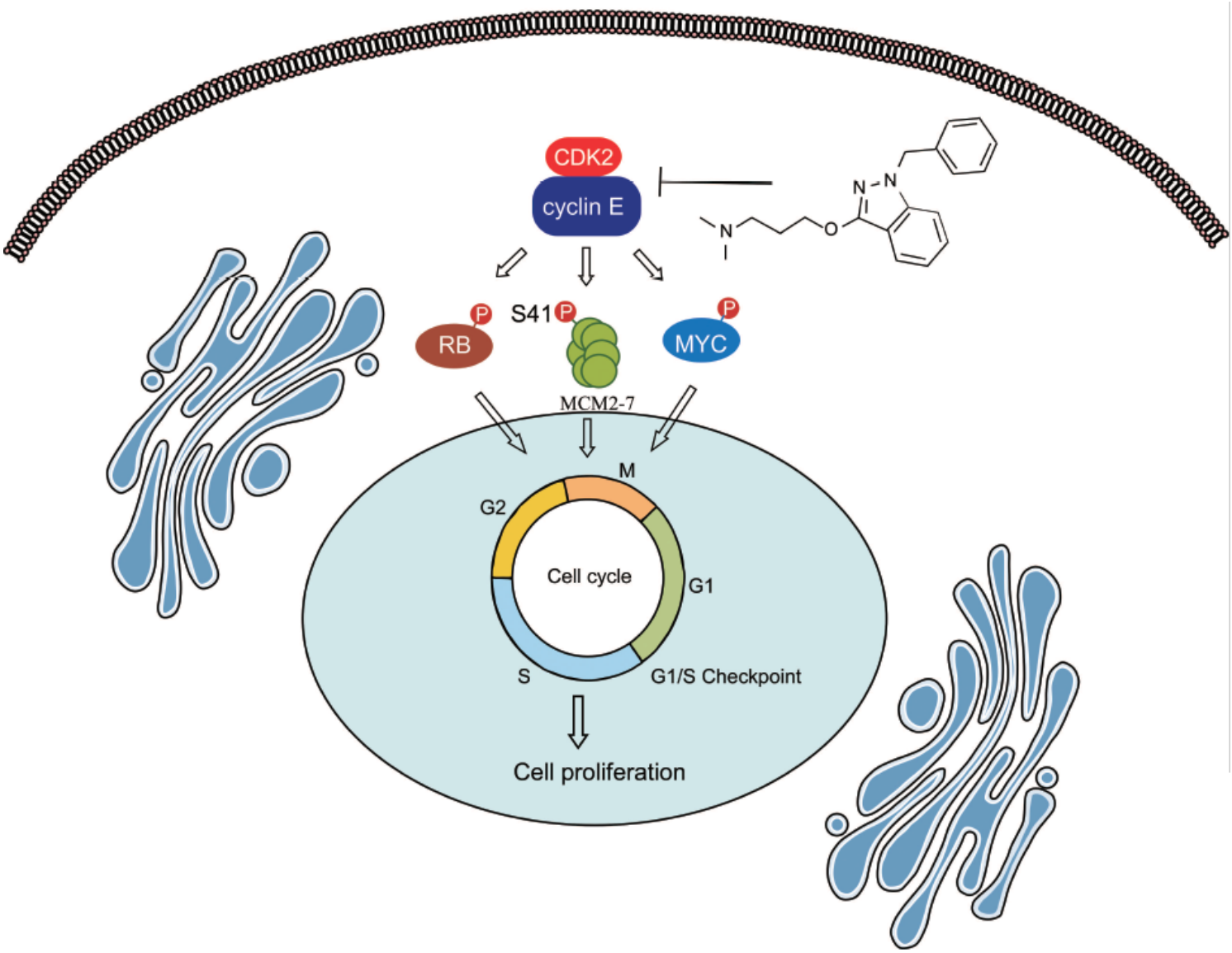

Figure 7

Molecular model of anti-tumor activity of benzydamine

Supplementary Files

This is a list of supplementary files associated with this preprint. Click to download.

- Supplementarymaterial1.doc
- Supplementarytable1.xls